Available online at www.sciencedirect.com
SCIENCE DIRECT®
Computers and Chemical Engineering 27 (2003) 1345–1360
Computers & Chemical Engineering
www.elsevier.com/locate/compchemeng

Optimization of semicontinuous emulsion polymerization reactions by IDP procedure with variable time intervals

P.H.H. Araújo, R. Giudici *

Departamento de Engenharia Química, Escola Politécnica da Universidade de São Paulo, 380 travessa 3 Av. Prof. Luciano Gualberto, 05508-900 São Paulo, SP, Brazil

Received 6 February 2003; accepted 7 February 2003

Abstract

Optimization of a semicontinuous emulsion polymerization reaction is carried out using a mathematical model derived from first principles to represent the process. Iterative Dynamic Programming (IDP), being a straightforward procedure that allows the implementation of optimization constraints, is an attractive tool to optimize highly complex and nonlinear equation systems such as those that are used to represent the emulsion polymerization processes. In order to minimize the reaction time of a semicontinuous reaction, time intervals with varying lengths were used allowing the establishment of the optimal operation conditions where the final time is not specified. The optimization procedure is applied to two emulsion polymerization systems: (a) butyl acrylate/vinyl acetate copolymerization with controlled composition; (b) vinyl acetate homopolymerization with specified molecular weight. Results show that significant reductions of reaction time are possible and that their extent depends on the reactor's heat removal capacity and on the formulated constraints.

Keywords: Dynamic optimization; Emulsion polymerization; Semicontinuous reactor

1. Introduction

Emulsion polymerization is a process of great industrial interest used to produce polymer via free radical in dispersed media. The global mechanism of polymerization in such a multiphase system is extremely complex due to process interactions that occur in each phase and diffusion mechanisms of the components between these phases. One of the main advantages of this process, due to its compartmentalized nature, is the possibility to obtain polymers of high molecular weight at high polymerization rates. On the other hand, the complexity of the system induces more intense difficulties on modeling, on-line measurements as well as control of the characteristics of the product.

The nonlinear characteristic of such systems and the complexity on modeling make the development of optimization procedures of emulsion polymerization reactions a very challenging task. Any optimization strategy to be implemented in an industrial polymerization reactor has to include the dynamics of reactor temperature control as the reaction is usually very exothermic and the reactor heat removal capacity is limited. Nevertheless, the complexity of the system increases when the dynamics of the reactor temperature control is included.

Semicontinuous reactors are often used to carry out strongly exothermic emulsion polymerization reactions. Usually, industrial operation does not take full advantage of the reactor heat removal capacity as the reaction conditions are often defined to control the peak of heat generation. Several articles in literature propose the use of optimal monomer feed profiles to reduce reaction time and to control polymer composition during semicontinuous emulsion polymerization reactions (Arzamendi, Leiza & Asua, 1991; Kozub & MacGregor, 1992; Canu, Canegallo, Morbidelli & Storti, 1994; Saldivar & Ray, 1997; among others). Nevertheless, these works are limited to isothermal reactions.

* Corresponding author. Tel.: +55-11-3091-2254; fax: +55-11-3813-2380.
E-mail address: rgiudici@usp.br (R. Giudici).

0098-1354/03/$ - see front matter © 2003 Published by Elsevier Science Ltd.
doi:10.1016/S0098-1354(03)00057-7

Nomenclature

Emulsion polymerization model

A	vinyl acetate
A_j	heat transfer area (cm^2)
A_{pT}	total particle surface area (cm^2)
a_s	area covered by 1 g mol of emulsifier (cm^2/gmol)
B	butyl acrylate
C_{inst}	instantaneous copolymer composition ratio
CMC	critical micelar concentration (g/cm^3)
$C_{pj,e}$	specific heat of reactor fees streams (cal/(g K))
C_{pwj}	specific heat of cooling fluid (cal/(g K))
D_p	diffusion coefficient in the polymer particles (cm^2/s)
D_w	diffusion coefficient in the aqueous phase (cm^2/s)
[E]	concentration of emulsifier in the reactor (g/cm^3)
$[E]_{ads}$	emulsifier adsorbed on polymer particles (g/cm^3)
$[E]_{ads}^{sat}$	emulsifier adsorbed on polymer particles at saturation (g/cm^3)
$[E]_{aq}$	concentration of emulsifier in the aqueous phase (g/cm^3)
f	initiator efficiency
F_i	feed rate of monomer i to the reactor in (mol/s)
f_{kam}	efficiency of radical entry rate into micelles
f_{ke}	efficiency of radical entry rate into polymer particles
$[I]$	concentration of initiator in the reactor (g/cm^3)
i	amount of monomer i (A or B) in the reactor (mol)
i_0	amount of monomer i in the initial charge of the reactor (mol)
i_{pol}	amount of monomer i in polymer particles (mol)
$[i]_{pol}$	concentration of monomer i in polymer particles (mol/cm^3)
j_{crit}	critical length of radical (homogeneous nucleation)
k'	coefficient of emulsifier adsorption by polymer particles
k_{am}	radical entry rate into micelles (cm^3/(mol s))
k_e	radical entry rate into polymer particles (cm^3/(mol s))
k_{fi}	average rate constant for chain transfer of radical type i in the polymer phase (cm^3/(mol s))
k_{fij}	rate constant for chain transfer of radical type i to monomer j in the polymer phase (cm^3/(mol s))
k_{fP}	average rate constant for chain transfer to polymer in the polymer phase (cm^3/(mol s))
k_{fPi}	rate constant for chain transfer of radical type i to copolymer in the polymer phase (cm^3/(mol s))
k_i	rate constant for initiator decomposition (1/s)
$k^p i$	partition coefficient of monomer i between aqueous phase and polymer phase
k_{pi}	average rate constant for propagation of radical type i in the polymer phase (cm^3/(mol s))
k_{pij}	rate constant for propagation of radical type i in with a radical type j in thepolymer phase (cm^3/(mol s))
k_{piaq}	average rate constant for propagation of radical type i in the aqueous phase (cm^3/(mol s))
k_t	average rate constant for termination in the polymer phase (cm^3/(mol s))
k_{taq}	average rate constant for termination in the aqueous phase (cm^3/(mol s))
k_{tij}	rate constant for termination of radical type i with radical type j in the polymer phase (cm^3/(mol s))
$[M_i]$	concentration of monomer i (A or B) in the reactor (g/cm^3)
$[M_i]_{aq}$	concentration of monomer i in the aqueous phase (g/cm^3)
$[M_i]_{pol}$	concentration of monomer i in the polymer phase (g/cm^3)
$\tilde{n}$	average number of radicals per polymer particle

The iterative dynamic programming (IDP) procedure is an attractive tool to optimize highly complex and nonlinear equation systems such as those of the emulsion polymerization processes as the procedure is straightforward and allows the implementation of optimization constraints. The IDP procedure was applied by Sayer, Arzamendi, Asua, Lima and Pinto (2001), to optimize the molecular weight distribution (MWD) and polymer composition during isothermal semicontinuous emulsion polymerizations, nevertheless reduction in reaction time was not attempted. Santos, Sayer, Lima and Pinto (1999) used the optimization procedure presented by Sayer et al. (2001) the differences of not computing the MWD and creating an external loop to minimize the reaction time. Nevertheless, this procedure requires an almost prohibitively long computational time, as the optimization procedure has to find the optimum solution for each reaction time.

According to Luus (1993), when the system is highly nonlinear, the global optimum solution may be difficult to obtain even when the final time is given. When the final time is free, there is an additional variable to be determined. Bojkov and Luus (1994, 1996) used stages of varying lengths in IDP, and observed that accurate switching times can be obtained, as is required for time-optimal control problems. By simultaneously searching for the stage lengths and also for the values for control, accurate control policies can be obtained with a small number of stages. It was also observed that the residence time for free final-time problems can be reduced substantially by incorporating the final time directly into the performance index. Another advantage of using variable time intervals is that it may reduce the number of intervals and so the computational effort, as intervals where there is almost no difference the best manipulated variables may be reduced to a single interval.

The optimization of polymerization processes may often present a conflicting criteria, as the minimization of reaction time and at the same time improving certain polymer qualities as average molecular weight or reaching high final conversion. This is the main motivation of several studies dealing with the use of multiobjective optimization for polymerization reactors (Tsoukas, Tirrell & Stephanopoulos, 1982; Choi & Butala, 1991; Gupta & Gupta, 1999; among others) as it may provide the achievement of all targets simultaneously. Nevertheless, according to Bhaskar, Gupta and Ray (2001), the multiobjective optimization of real-life systems is quite complex and each new application may require the development of several adaptations of optimization algorithms to obtain meaningful solutions, irrespective of which mathematical procedure is used for the purpose.

In this work, the operation of semicontinuous emulsion polymerization reactors is optimized. The optimization is performed by IDP procedure with variable time intervals and is based on a detailed process model derived from first principles. The major objective of these optimizations is to minimize the duration of the reaction time obtaining a polymer with a desired quality (composition profile or molecular weight) and, as this reaction is highly exothermic, taking the safety aspect into account. The aim is to determine the time evolution of the reacting mixture temperature and the feed rates of reactants that not only define a maximal efficiency but also involve an adequate heat generation to be removed by the cooling system. The optimization procedure is applied to vinyl acetate/butyl acrylate emulsion copolymerization and vinyl acetate emulsion homopolymerization. The conflicting criteria of reducing reaction time and at the same time achieving high final conversion as optimization objectives was minimized by establishing a high value for the weight factor of the final conversion. For the emulsion copolymerization case, it is also shown that forcing the feeding of the less reactive monomer in the first N intervals and using a NLA controller to calculate the flow rate of the more reactive monomer, eliminates the problem of introducing one more target into the objective function, in this case, the polymer composition. Results show that significant reductions of the reaction time are possible and that their extent depends on the reactor's heat removal capacity, on the desired polymer quality and on the formulated safety constraints.

2. Emulsion polymerization model

The kinetic mechanism used to represent the emulsion polymerization process considers the following reactions: initiation, propagation, transfers to monomer and to polymer and termination. The following assumptions are used to derive the model equations:

- kinetic constants in the aqueous and polymer phases are the same;
- kinetic constants do not depend on chain length;
- the pseudo-steady-state hypothesis is valid for radicals;
- radical propagation occurs both in the aqueous phase and inside the polymer particles;
- particles are generated by both homogeneous and micellar nucleation mechanisms;
- radicals that enter micelles or polymer particles are of length z to $jcrit-1$;
- radicals generated by initiation or chain transfer to monomer present similar reactivities;
- radical reactivity is given by the last monomeric unity;
- monomer concentration in the polymer particles, monomer droplets and aqueous phase are at thermodynamic equilibrium;

- the reactor operates non-isothermally;
- the global heat exchange coefficient changes with conversion;
- tank reactor is perfectly mixed;
- partition coefficients of the monomers are constant;
- critical micellar concentration (CMC) is constant.

The mass, the population and the energy balance equations used to describe the semicontinuous emulsion polymerization might be written as:

$$\frac{d(V_R[I])}{dt} = [I]_e q_e - k_I [I] V_R \tag{1}$$

$$\frac{d(V_R[W])}{dt} = [W]_e q_e \tag{2}$$

$$\frac{d(V_R[E])}{dt} = [E]_e q_e \tag{3}$$

$$\frac{d(V_R[M_i])}{dt} = q_e[M_i]_e - \frac{\tilde{n}N_P}{N_A}\, k_{pi}[M_i]_{pol} + [R_T]_{aq} V_{aq} k_{pi_{aq}}[M_i]_{aq} \tag{4}$$

$$\frac{d(V_R)[P]}{dt} = \frac{\tilde{n}N_P}{N_A} \sum_{i=A,B} k_{pi}[M_i]_{pol} + [R_T]_{aq} V_{aq} \times \sum_{i=A,B} k_{pi_{aq}}[M_i]_{aq} \tag{5}$$

$$y_A \frac{d(V_R[P])}{dt} + [P]\frac{d(V_R y_A)}{dt} = \frac{\tilde{n}N_P k_{pi}[M_A]_{pol}}{N_A}[R_T]_{aq} V_{aq} k_{pi_{aq}}[M_A]_{aq} \tag{6}$$

where $\tilde{n}$ is the average number of radicals per polymer particle, calculated as proposed by Hansen and Ugelstad (1978). Monomer concentration in the polymer particle, aqueous phase or polymer particles are calculated by the method proposed by Omi, Kushibiki, Negishi and Iso (1985) and are presented in Appendix A.

The following average coefficients are used to describe the copolymerization kinetics in the polymer particles and the coefficients for the aqueous phase are analogous:

Propagation:

$$k_{pi} = k_{pAi} P_{Ap} + k_{pBi} P_{Bp} \tag{7}$$

Chain transfer to monomer:

$$k_{fmi} = k_{fAi} P_{Ap} + k_{fBi} P_{Bp} \tag{8}$$

Chain transfer to polymer:

$$k_{fP} = k_{fPA} P_{Ap} + k_{fPB} P_{Bp} \tag{9}$$

Termination:

$$k_t = k_{tAA} P_{Ap}^2 + 2k_{tAB} P_{Ap} P_{Bp} + k_{tBB} P_{Bp}^2 \tag{10}$$

where P_{Ap} and P_{Bp} are the relative frequencies of radicals containing monomeric units of type A or B at the active end.

The emulsifier might be present in the aqueous phase, free or as a micelle, and also, might be adsorbed on the polymer particles surface or on the monomer droplets surface. As total monomer droplets surface is much lower than the polymer particles surface, it is possible to neglect the amount of emulsifier adsorbed on monomer droplets surface:

$$V_R[E] = V_{aq}[E]_{aq} + \beta N_{mic} + A_{pT}[E]_{ads} \tag{11}$$

$$\beta = \frac{4\pi r_m^2 P M_E}{a_s} \tag{12}$$

where A_{pT} represents the total polymer particle surface area and is calculated considering that all particles are spherical and of the same size.

Variables $[E]_{aq}$, $[E]_{ads}$ and N_{mic} must be computed for two different cases:

2.1. Case 1

Emulsifier concentration is above CMC-free emulsifier concentration in the aqueous phase is equal to CMC; emulsifier concentration adsorbed on polymer particles is equal to the saturation concentration ($[E]_{ads}^{sat}$) and the exceeding emulsifier is in the form of micelles:

$$[E]_{aq} = [E]_{CMC} \tag{13}$$

$$[E]_{ads} = [E]_{ads}^{sat} = \frac{P M_E}{a_s} \tag{14}$$

$$N_{mic} = \frac{1}{\beta}(V_R[E] - [E]_{CMC} V_{aq} - A_{p_T}[E]_{ads}^{sat}) \tag{15}$$

If N_{mic} is equal or lower than 0, emulsifier concentration is below CMC, then Case 2 conditions must be taken into account.

2.2. Case 2

Emulsifier concentration below CMC—no micelles are formed, it is assumed that the emulsifier is preferably absorbed on polymer particles stabilizing them. The fraction of particle surface area covered by the emulsifier is calculated by:

$$\theta_{ad} = \frac{k'[E]_{aq}}{1 + k'[E]_{aq}} \tag{16}$$

$$[E]_{ads} = \frac{P M_E \theta_{ad}}{a_s} \tag{17}$$

To calculate the radical balance in the aqueous phase, it is assumed that the pseudo-steady-state hypothesis is valid for these radicals. The critical length of a radical (j_{crit}) defines the point when a radical becomes insoluble in the aqueous phase generating a new polymer particle

(homogeneous nucleation). The critical length depends of the solubility of the monomer in the aqueous phase. A radical with length z is the smallest radical that can enter in a micelle or in a polymer particle (Gilbert, 1995). The total concentration of radicals in the aqueous phase is:

$$[R_T]_{aq} = \sum_{h=1}^{jcrit-1} [R_h]_{aq} \tag{18}$$

The concentration of the radicals with one momeric unit is:

$$[R_1]_{aq} = \frac{2fk_I[I] + \frac{\tilde{n}N_P}{N_A V_R}\sum_{i=A,B} k_{fmi}[M_i]_{pol}}{\sum_{i=A,B} k_{pi_{aq}}[M_i]_{aq} + \bar{k}_{t_{aq}}[R_T]_{aq}} \tag{19}$$

$\underline{\mathbf{h} = \mathbf{2}, \ldots, \mathbf{z-1}}$: the concentration of radicals of length between 2 and $z-1$ is given by:

$$[R_h]_{aq} = \frac{[R_{h-1}]_{aq}\sum_{i=A,B} k_{pi_{aq}}[M_i]_{aq}}{\sum_{i=A,B} k_{pi_{aq}}[M_i]_{aq} + \bar{k}_{t_{aq}}[R_T]_{aq}} = [R_{h-1}]_{aq}\alpha \tag{20}$$

Thus it is possible to obtain:

$$[R_{z-1}]_{aq} = [R_{z-2}]_{aq}\alpha = [R_1]_{aq}\alpha^{z-2} \tag{21}$$

$\underline{\mathbf{h} = \mathbf{z}, \ldots, \mathbf{jcrit-1}}$: the concentration of radicals of length between z and $jcrit-1$ is given by:

$$[R_h]_{aq} = \frac{[R_{h-1}]_{aq}\sum_{i=A,B} k_{pi_{aq}}[M_i]_{aq}}{\sum_{i=A,B} k_{pi_{aq}}[M_i]_{aq} + \bar{k}_{t_{aq}}[R_T]_{aq}\frac{(k_e N_P + k_{am}N_{mic})}{V_R N_A}} = [R_{h-1}]_{aq}\xi \tag{22}$$

The entry rates of radicals into particles and micelles are given by:

$$k_e = f_{ke}4\pi D_w N_A r_{ps} \tag{23}$$

$$k_{am} = f_{kam}4\pi D_w N_A r_m \tag{24}$$

Thus it is possible to obtain:

$$[R_h]_{aq} = [R_{z-1}]_{aq}\xi^{h-(z-1)} = [R_1]_{aq}\alpha^{z-2}\xi^{h-(z-1)} \tag{25}$$

$$[R_{jcrit-1}]_{aq} = [R_1]_{aq}\alpha^{z-2}\xi^{jcrit-z} \tag{26}$$

The total concentration of radicals in the aqueous phase is:

$$[R_T]_{aq} = [R_1]_{aq}\left(1 + \sum_{h=2}^{z-1}\alpha^{h-1} + \alpha^{z-2}\sum_{h=z}^{jcrit-1}\xi^{h-(z-1)}\right) \tag{27}$$

The total concentration of radicals in the aqueous phase that can enter a micelle or a particle is:

$$[R_T^{ent}]_{aq} = [R_1]_{aq}\alpha^{z-2}\sum_{h=z}^{jcrit-1}\xi^{h-(z-1)} \tag{28}$$

$[R_1]_{aq}$ and $[R_T]_{aq}$ are obtained by an iterative procedure.

The population balance gives the particle number evolution. Homogeneous and micellar nucleation were taken into account:

$$\frac{dN_P}{dt} = N_A V_{aq}[R_{jcrit-1}]_{aq}\sum_{i=A,B} k_{pi_{aq}}[M_i]_{aq} + k_{am}N_{mic}[R_T^{ent}]_{aq} \tag{29}$$

The average molecular weights of polymer with chain transfer to polymer are calculated by the method of the moments as presented in Appendix B.

The reactor and jacket temperatures are calculated with the equations of the energy balances. In these equations, only the main components (monomers A and B, polymer and water) are considered:

$$\frac{d\left[V_R\sum_{j=A,B,W,P}[M_j]C_{pj}(T_r - T_{ref})\right]}{dt} = \sum_{j=A,B,W} w_{j,e}q_e C_{pj,e}(T_e - T_{ref}) + \sum_{i=A,B}\left[\frac{\tilde{n}\cdot N_P}{N_A}(-\Delta H_{pi})k_{pi}[M_i]_{pol} \times [R_T]_{aq}V_{aq}(-\Delta H_{pi})k_{piaq}[M_i]_{aq}\right] - U_j A_j(T_r - T_j) - Q_{lR} \tag{30}$$

$$W_j\frac{d[C_{pwj}(T_j - T_{ref})]}{dt} = q_{je}C_{pwje}(T_{je} - T_{ref}) - q_{js}C_{pwj}(T_j - T_{ref}) - Q_{lj} - U_j A_j(T_j - T_r) \tag{31}$$

where T_{ref} is the reference temperature ($T_{ref} = 25\,^{\circ}C$), T_e is the inlet temperature of the reactants into the reactor ($T_e = 25\,^{\circ}C$), T_j is the jacket temperature and T_r is the reactor temperature. The global heat exchange coefficient (U_j) changes with conversion according to:

$$U_j(xg) = U_j(0) + (U_j(1) - U_j(0))xg^2 \tag{32}$$

It was considered that at 100% conversion the global heat transfer coefficient was 20% lower than at the beginning of the reaction ($U_j(1) = 0.80\,U_j(0)$). The same decrease of 20% in U_j was observed by Saenz de Buruaga (1998) for similar reaction conditions.

2.3. Temperature control

The thermal control of the semicontinuous reactor considered in this work is achieved by a jacket in which

the inlet temperature of a heating/cooling fluid is adjusted. In this case, the fluid is water and a PI controller calculates the inlet temperature. The PI controller adjusts T_{je} every 30 s, in order to control the reactor temperature and it was assumed that the inlet temperature changes immediately. It was considered that the temperature T_{je} cannot change more than 5 °C in 30 s. The cooling fluid inside the jacket was considered perfectly mixed.

2.4. Composition control

Latex must present strict specifications. One of the more important characteristics of polymers obtained by copolymerization is the composition of the formed polymer. Composition control becomes more complex when the reaction involves monomers with different water solubilities and reactivity ratios, as is the case of the system VA/BA where the reactivity ratios differ more than two orders of magnitude. In order to control the polymer composition, a non-linear adaptive (NLA) controller as proposed by Leiza, de la Cal, Meira and Asua (1993) was implemented. Two different monomer feed streams were used, one for each monomer. Knowing monomer concentrations in the reactor it is possible for the controller to adjust monomer ratio in the polymer particles in order to produce a copolymer of the desired composition calculating the flow rate of the more reactive monomer according to the following equations:

$$C_{inst} = \frac{R_{pA}}{R_{pB}} = \frac{r_A \cdot \dfrac{[A]_{pol}}{[B]_{pol}} + 1}{r_B \cdot \dfrac{[A]_{pol}}{[B]_{pol}} + 1} \tag{33}$$

Setting the desired instantaneous copolymer composition ratio (C_{inst}) for the whole reaction it is possible to calculate the monomer feed rate of the more reactive monomer by the ratio of the concentrations of the monomers A and B in the polymer particles ($\beta = [A]_{pol}/[B]_{pol}$).

$$\beta = \frac{-(C_{inst} - 1)\sqrt{(C_{inst} - 1)^2 + 4r_A r_B C_{inst}}}{2r_B C_{inst}} \tag{34}$$

The quantities of monomers A and B in the reactor are related to the quantities of monomer in the particles, $A_{pol} \times B_{pol}$, by the following equations:

$$A = A_{pol}(1 + V_{aq}/(V_{pol}k_A^p)) \tag{35}$$

$$B = B_{pol}(1 + V_{aq}/V_{pol}k_B^p) \tag{36}$$

Combination of Eqs. (35) and (36) gives the relation between B/A and β:

$$\frac{B}{A} = \frac{k_A^p}{k_B^p}\left(\frac{V_{pol}k_B^p + V_{aq}}{V_{pol}k_A^p + V_{aq}}\right)\beta \tag{37}$$

The material balances for monomers A and B can be approximated by the following difference equations:

$$\Delta A = A - A_0 = (F_A - R_{pA})\Delta t \tag{38}$$

$$\Delta B = B - B_0 = (F_B - R_{pB})\Delta t \tag{39}$$

Combination of Eqs. (38) and (39) gives:

$$\frac{A}{B} = \frac{A_0 + (F_A - R_{pA})\Delta t}{B_0 + (F_B - R_{pB})\Delta t} \tag{40}$$

From Eq. (40) an explicit algebraic equation for the flow rate of the more reactive monomer (F_B) can be obtained:

$$F_B = \frac{A_0}{\Delta t}\left(\frac{B}{A}\right) + (F_A - R_{pA})\left(\frac{B}{A}\right) - \frac{B_0}{\Delta t} + R_{pB} \tag{41}$$

3. Optimization procedure

The optimizations are performed through manipulation of decision variables along the reaction in order to approach a set of process objectives as close as possible. In this work, feed rates of different process streams, the length of each interval and temperature profile are the manipulated variables. Process objectives are polymer properties and the minimization of reaction time, respecting safety aspects along the whole reaction. Both manipulated variables and process objectives must satisfy certain process constraints. The optimization procedure was applied to two examples: (a) butyl acrylate/vinyl acetate copolymerization with controlled composition; (b) vinyl acetate homopolymerization with specified molecular weight. Each example has it owns particularities as will be explained in the next section.

The continuous dynamic system is described by the following system of differential–algebraic equations:

$$\frac{d\underline{x}}{dt} = \underline{f}(\underline{x}, \underline{u}) \tag{42}$$

$$\underline{x} = \underline{g}(\underline{x}, \underline{u}) \tag{43}$$

where $\underline{x}$ is a state vector ($n \times 1$) and $\underline{u}$ is a manipulated variables vector ($m \times 1$) to be optimized bounded by:

$$\alpha_i \le u_i \le \beta_i \quad i = 1, \ldots, m \tag{44}$$

Process constraints may be treated as penalty functions, resulting in an augmented objective function. According to Luus and Rosen (1991) this way to treat the constraints is convenient because in the IDP procedure the objective function does not have to be differentiable, and, consequently, a wide range of choices might be used as penalty functions. The problem

than consists of the determination of profiles $u_i(t)$ in the time interval $[t_{k-1}, t_k]$, in order to minimize the objective function. Optimizations are performed by IDP procedure (Luus, 1998). The IDP might be implemented if the process time period is divided into several intervals and integration of the process model is performed only in those time intervals that are affected by the change of the manipulated variables under consideration. The optimization algorithm, as applied in this work, is presented below.

3.1. Optimization algorithm

The IDP algorithm with variable time intervals can be summarized in major steps:

1) Choose the number of time intervals where all the monomer is fed to the reactor (N), for the copolymerization case, only the less reactive monomer is completely fed. The amount of monomer fed in each one of the N intervals is the same, but the length of the time of each interval is variable. Choose the number of intervals after the monomer addition to complete the reaction (P). If the process is the copolymerization reaction with controlled composition the more reactive monomer may be added also in the last P intervals.
2) Choose the number of optimization iterations (*iter*), the random combinations (A) for manipulated variables (u_i), the initial profiles for u_i, the size of initial search area (r_i) for each manipulated variable (the size may also change according to the interval, N or P) and the contraction factor of the search area (λ).
3) Using initial u_i of step 2, integrate system from $t=0$ to $t=t_f$ $(N+P)$ to generate trajectories of x, storing the initial values of x at each time interval k, in such a way that the values of $x(k-1)$ correspond to the values of x at the beginning of interval k.
4) Starting at the last interval $(N+P)$, integrate equations from t_f $(N+P-1)$ to $t_f(N+P)$, using as initial states $x(N+P-1)$ either of step 3 (only in the first iteration) or of the previous iteration. Repeat the procedure for each combination A of u. Choose $u(N+P)$ that resulted in the lowest value of the objective function and store it to use in step 5.
5) Go to interval $N+P-1$. For each combination of $u(N+P-1)$ integrate equations from $t_f(N+P-2)$ to $t_f(N+P)$, using as initial states $x(N-P-2)$ of step 3 (or of the previous iteration). Continue integration until $t=t_f(N+P)$ using at this interval the value of $u(N+P)$ of step 4. Choose $u(N+P-1)$ that resulted in the lowest value of the objective function and store it to use in step 6. Repeat the procedure until reaching interval 1, corresponding to initial time $t=0$. Store trajectory x.
6) Reduce the size of the allowable region for the manipulated variables: $r_i(^{j+1}) = \lambda \cdot r_i(^{j})$ where j is the iteration index. Use u of step 5 stored as the manipulated variables that gave the best results for the objective function as initial value of u in each interval and also as the midpoints for the next iteration. Increment the iteration index by 1 and go back to step 4. Continue the procedure for a specified number of iterations (*iter*) and examine the results.

The program is implemented in FORTRAN and the system of differential and algebraic equations of the emulsion polymerization model is solved with the numerical integrator DASSL (Petzold, 1982). Typical computation time for the off-line optimization problems here treated varied from a few to several hours (in a PC 400 MHz, 128 MB RAM), mostly depending on the operating conditions and the initial estimates of the decision variable vector.

4. Results and discussion

The optimization procedure is applied to two semi-continuous emulsion polymerization systems: (a) butyl acrylate (BA)/vinyl acetate (VA) copolymerization with controlled composition; (b) vinyl acetate homopolymerization with specified molecular weight.

4.1. Case A: butyl acrylate/vinyl acetate copolymerization with controlled composition

The production of copolymers with homogeneous compositions (50/50 in molar basis) along the whole reaction with a maximum conversion at a minimum reaction time was considered in this dynamic optimization. To allow the control of copolymer composition, two different process feed streams were used. The first process stream contained the less reactive monomer (in this case, VA) which partially controls the reaction rate, and therefore, the reaction length, and the second one contained the more reactive monomer (BA), which controls the composition along the reaction. The composition control along the reaction is important to improve the homogeneity of the final polymer material. The mathematical model describing the VA/BA emulsion copolymerization was validated previously (Araújo & Giudici, 2001) with experimental data from Araujo (1997).

In order to carry out the optimization, the process was divided into four discrete time intervals. During the first two intervals (N intervals) the less reactive monomer is fed to the reactor and at the last intervals (P intervals) this feed rate is set equal 0. The more reactive monomer is fed according to the NLA controller during

all intervals in order to keep a constant polymer composition. The manipulated variables in the first two intervals (N) are the temperature profile (reactor temperature set-point profile for the PI controller) and the flow rate of the less reactive monomer (varying the length of each interval) and in the last P intervals the temperature profile and the length of each interval.

In order to ensure that all reactions would present the same final particle size distribution (this is an usual requirement of latex producers) the first reaction step (particle nucleation step or seed production step) was not optimized. Therefore, reaction optimization started 5 min after reaction beginning when polymer particle nucleation had already ceased. Initiator, emulsifier and water composed the initial charge of the reaction and were not fed during the reaction.

The process objectives, reduction of reaction time and high final conversion, were inserted into the objective function as:

$$F = w_1\left[\frac{t_f - t_f^d}{t_f^d}\right]^2 + w_2\left[\frac{xg_f - xg_f^d}{xg_f^d}\right] + w_3 R \qquad (45)$$

When the reaction temperature reaches 72 °C (at any point of the whole reaction), that is the boiling point of vinyl acetate at atmospheric pressure, R assumes a value equal 1, otherwise it remains equal 0. As the weight pondering (w_3) is very high when compared with the other weight factors, the objective function assumes a very high value and the value is rejected as the optimal result. For numerical calculations, the following values were assigned for the weights in Eq. (45): $w_1 = 2$; $w_2 = 10$; and $w_3 = 1000$.

The first two terms of the right hand side of the objective function (Eq. (45)) are inversely related to each other, as the reduction in reaction time may reduce final conversion and a great increase in the weight factor that ponders the final polymer conversion (w_2) may increase the reaction time. For this reason, it is necessary to find an adequate trade-off between these terms. To minimize this problem, if a pre-specified final conversion (99%) is reached at a time $t_{new} < t_{final}$, t_{final} is set equal t_{new}. The weight pondering the conversion (w_2) is higher than that pondering the final time (w_1), since it is more important to reach the specified final conversion than reducing the reaction time. Once the desired final conversion is reached the optimization drives to a more efficient reduction of the reaction time.

In this example, feeding all the less reactive monomer in the first N intervals and using the NLA controller to calculate the flow rate of the more reactive monomer, eliminates the problem of introducing one more target in the objective function, in this case, the polymer composition. This procedure presents an alternative to other works, like for instance Sayer et al. (2001), that introduced the polymer composition in the objective function.

In order to initialize the IDP procedure, initial values must be assigned for the duration of each interval and for the temperature profile. The initial feed rate profile of the less reactive monomer was assumed to be constant and low enough to ensure starved conditions. The temperature profile was assumed to be constant throughout the polymerization reaction and equal to the temperature used to produce the polymer particle seeds. Such initial conditions (constant temperature profile and starved conditions) would lead to a constant polymer composition, although it would also lead to an almost prohibitively high reaction time.

Kinetic constants and other parameters used in the following optimizations are presented in tables C.1 and C.2 (in Appendix C). Initial reaction conditions of vinyl acetate/butyl acrylate emulsion copolymerization are presented in Table 1:

Figs. 1 and 2 present results obtained at the initial conditions of the optimization procedure. The reaction temperature was set equal to 60 °C and the total reaction time was of 240 min. It can be observed that the instantaneous conversion is very high (~90%) during the reaction and that the copolymer composition was kept constant at 50/50 in molar basis (Fig. 1). Due to the high instantaneous conversion observed, the BA feed flow rate profile calculated by the NLA controller stays almost constant during VA feed period (Fig. 2).

Table 2 presents the optimization parameters used in this investigation, in accordance with the algorithm.

Figs. 3–5 present results obtained after the optimization. A significant reduction in reaction time, from 240 to 33 min, was observed with no remarkable prejudicial effect on final conversion and copolymer composition (Fig. 3). The dynamics of jacket and reactor temperatures are presented at Fig. 4, where the inlet jacket temperature is calculated by the PI controller and the desired reactor temperature (T_{rd}) is calculated by the optimization algorithm. During the first interval, T_{rd} was kept at 69 °C to respect the temperature constraint (reaction temperature (T_r) < 72 °C) as there was a small overshoot in T_r. At the other intervals T_{rd} assumes the maximum allowable value (70 °C). This behavior is caused by the high heat exchange capacity of a lab scale

Table 1
Reaction conditions

Variable	Value
Initial temperature (°C)	60.0
Total monomer fraction (w/w)	0.33
Water (g)	870.0
Emulsifier-sodium dodecyl sulfate (g)	2.0
Initiator-sodium persulfate (g)	2.0

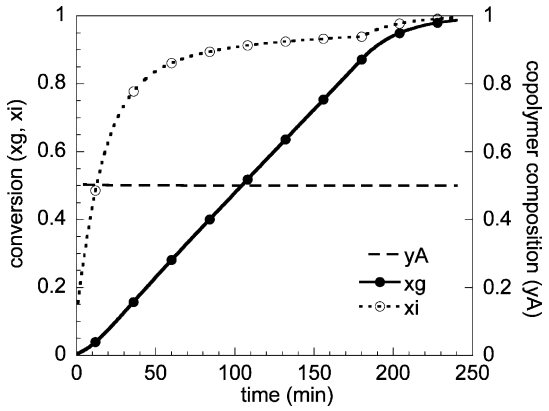

Fig. 1. Initial conditions of the optimization procedure: global conversion (xg); instantaneous conversion (xi); and molar fraction of vinyl acetate in the copolymer (yA).

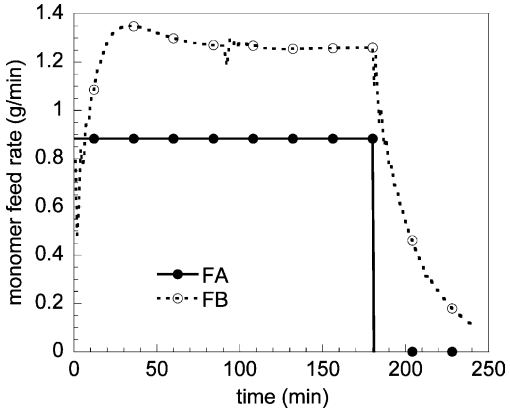

Fig. 2. Initial conditions of the optimization procedure: vinyl acetate (FA) and butyl acrylate (FB) feed rate.

reactor (considered in this case) when compared with an industrial reactor.

4.2. Case B: vinyl acetate homopolymerization with specified molecular weight

The optimization procedure was applied to vinyl acetate emulsion polymerization under industrial-like conditions, which includes constraints normally found in the operation of large-scale industrial reactors, such as maximum allowed reaction temperature and maximum total adiabatic temperature. The aim in this case is to maximize the productivity, i.e. to minimize the reaction time and to obtain a polymer with a desired molecular weight, taking safety aspects into account. The mathematical model was validated previously with

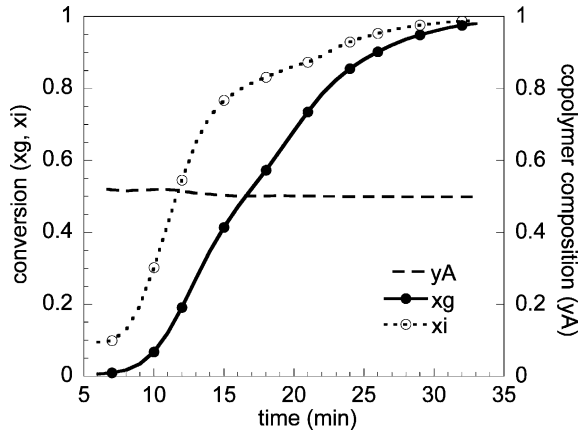

Fig. 3. Optimization results: global conversion (xg); instantaneous conversion (xi); and molar fraction of vinyl acetate in the copolymer (yA).

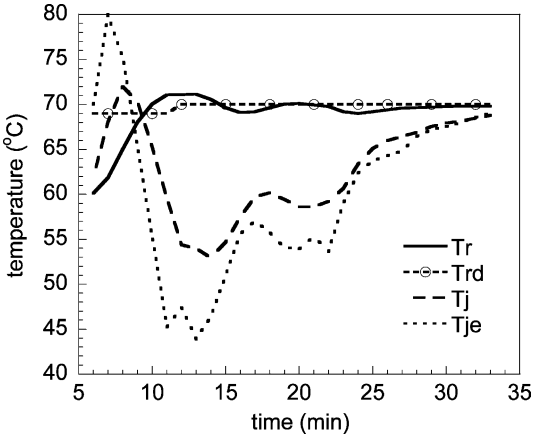

Fig. 4. Optimization results. Temperature profiles: reactor temperature (Tr); jacket temperature (Tj); desired reactor temperature (Trd); and inlet jacket temperature (Tje).

experimental data of vinyl acetate emulsion homopolymerization reaction obtained by Penlidis (1986).

Initiator and monomer feed flow rates and temperature profiles are chosen as the control variables. Temperature and initiator concentration increases accelerate the polymerization process, but may also reduce the molecular weight. When high molecular weight is desired, a compromise between production and product quality may be attained. In polymerizations of monomers that present a high rate of radical transfer to polymer, such as vinyl acetate, the molecular weight is also modified by the monomer feed flow profile. This occurs because the monomer feed profile changes the

Table 2
Optimization parameters

Number of iterations	Number of intervals	Contraction factor	Random combinations	Set-point range (°C)	Time range (min)
6	4	0.9	32	50–70	2–90

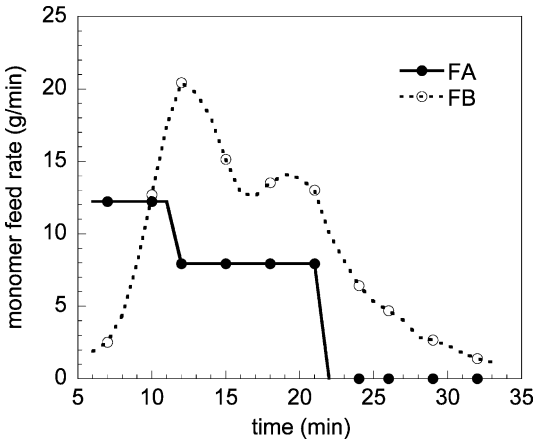

Fig. 5. Optimization results: vinyl acetate (FA) and butyl acrylate (FB) feed rate profiles.

monomer concentration in the polymer particles and then modifies the rate of transfer to polymer.

Reactions were always started at the same conditions (reaction temperature and reactant concentrations) and proceeded until polymer particle nucleation ceased. In this case, 10% of the total amount of vinyl acetate is added to produce the polymer seeds. Just after that point, in this case 35 min, the optimization procedure was started. This procedure is normally employed at industry in order to ensure that all reactions present the same particle size distribution. Kinetic constants and other parameters used in the following optimizations are presented in Tables C.1 and C.2 (in Appendix C). Initial reaction conditions of vinyl acetate emulsion polymerization are presented in Table 3.

Penalties factors applied to the objective function (Eq. (46)) are functions of the overall values at the end of the reaction as conversion, final reaction time, number and weight average molecular weight. To keep the safety of the operation a constraint was also applied in the objective function when the reactor temperature reaches 80 °C and/or the total adiabatic temperature reaches 100 °C. If one of these conditions is not satisfied R assumes a value equal 1, otherwise it remains equal 0.

Table 3
Reaction conditions

Variable	Value
Initial temperature (°C)	50.0
Total monomer fraction (w/w)	0.53
Water (kg)	9000.0
Emulsifier-sodium dodecyl sulfate (kg)	60.0
Initiator-sodium persulfate (kg)	30.0

$$F = w_1\left[\frac{t_f - t_f^d}{t_f^d}\right]^2 + w_2\left[\frac{x_f - x_f^d}{x_f^d}\right] + w_3\left[\frac{Mn_f - Mn_f^d}{Mn_f^d}\right]^2 + w_4\left[\frac{Mw_f^d - Mw_f^d}{Mw_f^d}\right] + w_5\mathrm{R} \quad (46)$$

In order to carry out the optimization, the process was divided into five discrete time intervals. During the first four intervals monomer is continuously fed to the reactor and at the last interval monomer feed rate is set equal 0. Initiator was only allowed to be fed in the last interval to complete the reaction. The amount of monomer fed in each of the four feed intervals is the same, but the feed rate changes with the length of each interval. At the initial operation conditions monomer feed rate was constant and low to ensure starved conditions. Initiator was not fed after monomer addition. Temperature was set constant throughout the polymerization and equal to the temperature used to produce the polymer particle seeds. Such initial conditions (low temperature and starved conditions) lead to an extremely high molecular weight, nevertheless they also lead to a high reaction time. The objective is to reduce reaction time keeping the high molecular weight ($\sim 6 \times 10^6$) obtained with the initial operational conditions (50 °C and 400 min of reaction time). For numerical calculations, the following values were assigned for the weights in Eq. (46): $w_1 = 2$; $w_2 = 10$; $w_3 = 1$; $w_4 = 10$; and $w_5 = 1000$. Table 4 presents the optimization parameters used in this investigation, in accordance with the algorithm.

Fig. 6 shows the optimization results for conversion and molecular weight. Reaction time was drastically reduced as a high overall heat transfer coefficient was used and the weight average molecular weight reached 6×10^6. In Fig. 6 it might also be observed that while Mw increase significantly with conversion Mn remains almost constant. This behavior of the number and weight average molecular weights is typical of systems that present high transfer to polymer rates. The oscillations observed in the instantaneous conversion are due to the increase in vinyl acetate feed rate.

Fig. 7 shows the evolutions of the temperatures (reactor temperature, desired reactor temperature, jacket temperature, total adiabatic temperature) along the reaction. During the first interval (until 70 min) the reaction was kept at medium temperature (60 °C) to increase the molecular weight and after that the temperature continuously raised to complete the reaction. At the fourth interval the temperature was limited by the total adiabatic temperature that almost reached 100 °C. When a much lower overall heat transfer coefficient was used higher reaction time was needed. Since the global energy balance of the reactor and the limitations of the heat removal capacity of the reactor are taken into account, it becomes straightforward to

Table 4
Optimization parameters

Number of iterations	Number of intervals	Contraction factor	Random combinations	Set-point range (°C)	Amount of initiator (kg)	Time range (min)
6	5	0.9	64	50–80	15	2–90

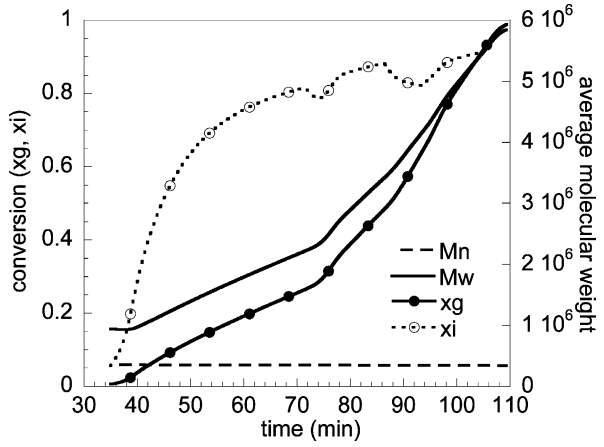

Fig. 6. Optimization results: overall conversion (xg), instantaneous conversion (xi), number (Mn) and weight (Mw) average molecular weight.

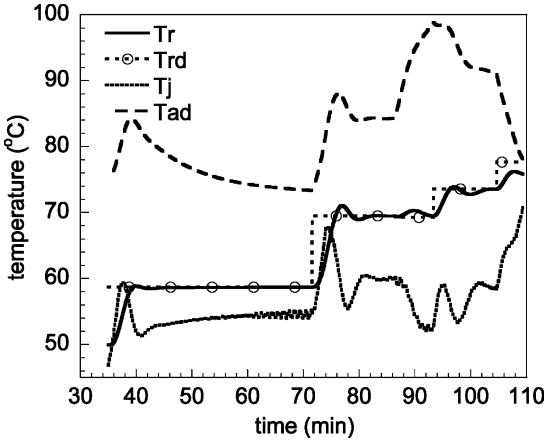

Fig. 7. Optimization results. Temperature profiles: reactor temperature (Tr); desired reactor temperature (Trd); jacket temperature (Tj); total adiabatic temperature (Tad).

predict operation conditions of large industrial reactors, and therefore, reducing scale-up problems.

Fig. 8 presents the optimization results for vinyl acetate and initiator feed rates. It is important to notice that initiator was only fed in the last interval when the monomer feed rate was set equal 0 and that the feed rate of initiator corresponds to the maximum amount of initiator allowed for each interval. In this example, initiator was only allowed to be fed in the last interval (part of the initiator was fed at the beginning of the reaction) and its function was to accelerate the reaction

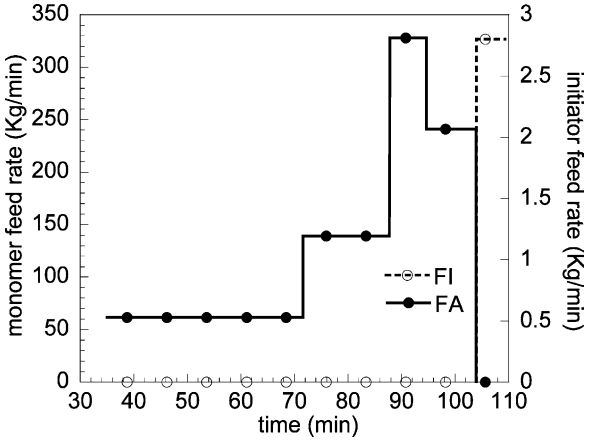

Fig. 8. Optimization results: monomer (FA) and initiator (FI) feed rates.

and to reduce the residual monomer content after the monomer addition.

5. Conclusions

In order to minimize the reaction time of a semi-continuous reaction, the use of time intervals of varying lengths was applied in IDP allowing the establishment of the optimal operation conditions where the final time is not specified. IDP has showed to be a straightforward procedure that allows the implementation of optimization constraints and to optimize highly complex and nonlinear equation systems such as those that are used to represent the emulsion polymerization processes.

The mathematical model used to represent the emulsion polymerization reactions was based on a detailed process model derived from first principles. The global energy balance of the reactor included the balance of the jacket allowing the development of optimal strategies that take the limitations of the heat removal capacity of the reactor into account.

The conflicting criteria of reducing reaction time and at the same time achieving high final conversion as optimization objectives was minimized by establishing a high value for the weight factor of the final conversion. For the emulsion copolymerization case, it is also shown that forcing the feeding of the less reactive monomer in the first N intervals and using a NLA controller to calculate the flow rate of the more reactive monomer, eliminates the problem of introducing one more target

into the objective function, in this case, the polymer composition.

Results show that the optimization procedure was able to minimize the reaction time and, simultaneously, obtaining a polymer with a desired quality (composition or molecular weight) and taking the safety aspect into account. The reductions of the reaction time were significant and their extent depends on the reactors heat removal capacity on the desired polymer quality (composition or molecular weight) and on the formulated safety constraints.

Acknowledgements

The PROFIX fellowship of CNPq for P.H.H. Araújo and the financial support from Conselho Nacional de Desenvolvimento Científico e Tecnológico (CNPq), and Fundação de Amparo à Pesquisa do Estado de São Paulo (FAPESP) are gratefully appreciated.

Appendix A: Monomer concentrations in the different phases

Using the partition coefficients of the monomers:

$$k_i^d = \frac{v_i^d / v_d}{v_i^{aq} / v_{aq}} \tag{A1}$$

$$k_i^{pol} = \frac{v_i^{pol} / v_{pol}}{v_i^{aq} / v_{aq}} \tag{A2}$$

where monomer volumes in monomer drops (v_i^d) and in the aqueous phase(v_i^{aq}) may be written as:

$$v_i^d = \frac{v_d}{v_{pol}} \frac{k_i^d}{k_i^{pol}} \; v_i^{pol} \tag{A3}$$

$$v_i^{aq} = \frac{v_{aq}}{v_{pol}} \frac{1}{k_i^p} \; v_i^{pol} \tag{A4}$$

The total volume of monomer i (v_i) is given by:

$$v_i = v_i^d + v_i^{pol} + v_i^{aq} \tag{A5}$$

$$v_i^{pol} = \frac{v_i}{1 + \dfrac{v_{aq}}{v_{pol} k_i^{pol}} + \dfrac{v_{aq} k_i^d}{v_{pol} k_i^{pol}}} \tag{A6}$$

$$v_d = \sum_{i=A,B} v_i^d \tag{A7}$$

$$v_{aq} = \sum_{i=A,B} v_i^{aq} + v_w \tag{A8}$$

$$v_{pol} = \sum_{i=A,\,B} v_i^{pol} + v_{copol} \tag{A9}$$

where v_w is the volume of water and v_{copol} is the volume of copolymer. Knowing v_i, v_{copol}, v_w, k_i^d and k_i^{pol}, it is possible to obtain v_i^d, v_i^{aq} and v_i^{pol} by the following iterative procedure:

1) set initial values for v_d, v_{aq} and v_{pol};
2) calculate v_i^{pol} with Eq. (A6);
3) calculate v_i^d and v_i^{aq} with Eqs. (A3) and (A4);
4) calculate the new values of v_d, v_{aq} and v_{pol} with Eqs. (A7), (A8) and (A9);
5) return to step 1 with the new values of v_d, v_{aq} and v_{pol} until convergence.

Once the volumes of each monomer in each phase (j) are known, the concentrations are calculated by:

$$[M_i]_j = \frac{v_i^j}{v_j} \frac{PM_i}{\rho_i} \tag{A10}$$

Appendix B: Set of equations used to calculate average molecular weights of polymer with chain transfer to polymer

Balance of radicals:

$$\begin{aligned}\frac{dR_1}{dt} = &-R_1 \sum_{i=A,B} k_{pi}[i]_{pol} - R_1 \sum_{i=A,B} k_{fmi}[i]_{pol} \\ &- \left[\frac{k_{fP}}{Na \cdot v_p} \sum_{n=1}^{\infty} nM_n\right] R_1 + \left[\sum_{i=A,B} k_{fmi}[i]_{pol}\right] \\ &\times \sum_{n=1}^{\infty} R_n + \left[\frac{k_{fP}}{Nav_p} M_1\right] \sum_{n=1}^{\infty} R_n - \left[\frac{k_t}{Na \cdot v_p}\right] \\ &\times \sum_{n=1}^{\infty} R_n R_1 + k_{abs} \\ = &\; 0\end{aligned} \tag{B1}$$

$$\begin{aligned}\frac{dR_n}{dt} = &+R_{n-1} \sum_{i=A,B} k_{pi}[i]_{pol} - R_n \sum_{i=A,B} k_{pi}[i]_{pol} - R_n \\ &\times \sum_{i=A,B} k_{fmi}[i]_{pol} - \left[\frac{k_{fP}}{Nav_p} \sum_{n=1}^{\infty} nM_n\right] R_n \\ &+ \left[\frac{k_{fP}}{Nav_p} nM_n\right] \sum_{n=1}^{\infty} R_n - \left[\frac{k_t}{Nav_p}\right] \sum_{n=1}^{\infty} R_n R_n \\ = &\; 0\end{aligned} \tag{B2}$$

$$\mu_k = \sum_{n=1}^{\infty} n^k R_n \tag{B3}$$

$$Q_k = \sum_{n=1}^{\infty} n^k M_n \tag{B4}$$

$$\left[\sum_{i=A,B} k_{pi}[i]_{pol}\right]\sum_{n=1}^{\infty}(n+1)^k R_n + \left[\sum_{i=A,B} k_{fmi}[i]_{pol}\right] + \mu_0 + abs + \left[\frac{k_{fP}}{Nav_p}\sum_{n=1}^{\infty} n^{k+1}M_n\right]\mu_0 = \left[\sum_{i=A,B} k_{pi}[i]_{pol}\right]\sum_{n=1}^{\infty} n^k R_n + \left[\sum_{i=A,B} k_{fmi}[i]_{pol}\right] \times \sum_{n=1}^{\infty} n^k R_n + \left[\frac{k_{fP}}{Nav_p} Q_1\right]\sum_{n=1}^{\infty} n^k R_n + \left[\frac{k_t}{Nav_p}\right]\mu_0 \times \sum_{n=1}^{\infty} n^k R_n \quad \text{(B5)}$$

$$\sum_{n=1}^{\infty} n^k R_{n-1} = \sum_{n=1}^{\infty}(n+1)^k R_n \quad \text{(B6)}$$

$$\text{for } k=0 \Rightarrow \sum_{n=1}^{\infty} R_n = \mu_0 \quad \text{(B7)}$$

$$\text{for } k=1 \Rightarrow \sum_{n=1}^{\infty}(n+1)R_n = \sum_{n=1}^{\infty} nR_n + \sum_{n=1}^{\infty} R_n = \mu_1 + \mu_0 \quad \text{(B8)}$$

$$\text{for } k=2 \Rightarrow \sum_{n=1}^{\infty}(n+1)^2 R_n = \sum_{n=1}^{\infty} n^2 R_n + 2\sum_{n=1}^{\infty} nR_n + \sum_{n=1}^{\infty} R_n = \mu_2 + 2\mu_1 + \mu_0 \quad \text{(B9)}$$

$$k=0 \Rightarrow \mu_0 = \sqrt{\frac{absNav_p}{k}} \quad \text{(B10)}$$

$$k=1 \Rightarrow \mu_1 = \frac{\left[\sum_{i=A,B} k_{pi}[i]_{pol}\right]Nav_p\mu_0 + \left[\sum_{i=A,B} k_{fmi}[i]_{pol}\right]Nav_p\mu_0 + [k_{fP}Q_2]\mu_0 + absNav_p}{\left[\sum_{i=A,B} k_{fmi}[i]_{pol}\right]Nav_p + k_{fP}Q_1 + k_t\mu_0} \quad \text{(B11)}$$

$$k=2 \Rightarrow \mu_2 = \frac{\left[\sum_{i=A,B} k_{pi}[i]_{pol}\right]Nav_p(\mu_0 + 2\mu_1)\left[\sum_{i=A,B} k_{fmi}[i]_{pol}\right]Nav_p\mu_0 + [k_{fP}Q_3]\mu_0 + absNav_p}{\left[\sum_{i=A,B} k_{fmi}[i]_{pol}\right]Nav_p + [k_{fP}Q_1] + k_t\mu_0} \quad \text{(B12)}$$

Balance of inactive polymer chains:

$$\frac{dM_n}{dt} = +\left[\sum_{i=A,B} k_{fmi}[i]_{pol}\right]R_n + \left[\frac{k_{fP}}{Nav_p}\sum_{n=1}^{\infty} nM_n\right]R_n - \left[\frac{k_{fP}}{Nav_p} nM_n\right]\sum_{n=1}^{\infty} R_n + \left[\frac{k_{tc}}{2Nav_p}\right]\sum_{l=1}^{n-1} R_l R_{n-l} + \left[\frac{k_{td}}{Nav_p}\right]\sum_{n=1}^{n} R_n R_n \quad \text{(B13)}$$

$$\sum_{n=1}^{\infty} n^k \frac{M_n}{dt} = \frac{d\sum_{n=1}^{\infty} n^k M_n}{dt} = \frac{dQ_k}{dt} \quad \text{(B14)}$$

$$\frac{dQ_k}{dt} = +\left[\sum_{i=A,B} k_{fmi}[i]_{pol}\right]\sum_{n=1}^{\infty} n^k R_n + \left[\frac{k_{fP}}{Nav_p} Q_1\right] \times \sum_{n=1}^{\infty} n^k R_n - \left[\frac{k_{fP}}{Nav_p}\mu_0\right]\sum_{n=1}^{\infty} n^{k+1}M_n + \left[\frac{k_{tc}}{2Nav_p}\right] \times \sum_{n=1}^{\infty} n^k \sum_{l=1}^{n-1} R_l R_{n-l} + \left[\frac{k_{td}}{Nav_p}\right]\mu_0\sum_{n=1}^{n} n^k R_n \quad \text{(B15)}$$

$$\sum_{n=1}^{\infty} n^k \sum_{l=1}^{n-1} R_l R_{n-1} = \sum_{n=1}^{\infty} R_n \sum_{l=1}^{\infty}(n+l)^k R_l \quad \text{(B16)}$$

$$\text{for } k=0 \Rightarrow \sum_{n=1}^{\infty} R_l \sum_{l=1}^{\infty} R_n = \mu_0^2 \quad \text{(B17)}$$

$$\text{for } k=1 \Rightarrow \sum_{n=1}^{\infty} R_n\left(\sum_{l=1}^{\infty} nR_l + \sum_{l=1}^{\infty} lR_n\right) = 2\mu_0\mu_1 \quad \text{(B18)}$$

$$\text{for } k=2 \Rightarrow \sum_{n=1}^{\infty} R_n\left(\sum_{l=1}^{\infty} n^2 R_l + 2\sum_{l=1}^{\infty} nlR_n + \sum_{l=1}^{\infty} l^2 R_l\right) = 2(\mu_0\mu_2 + \mu_1^2) \quad \text{(B19)}$$

$$\text{for } k=0 \Rightarrow \frac{dQ_0}{dt} = +\left[\sum_{i=A,B} k_{fmi}[i]_{pol}\right]\mu_0 + \left[\frac{k_{tc}}{2Nav_p}\right]\mu_0^2 + \left[\frac{k_{td}}{Nav_p}\right]\mu_0^2 \quad \text{(B20)}$$

$$k=1 \Rightarrow \frac{dQ_1}{dt} = +\left[\sum_{i=A,B} k_{fmi}[i]_{pol}\right]\mu_1 + \left[\frac{k_{fP}}{Nav_p}\ Q_1\right]\mu_1 - \left[\frac{k_{fP}}{Nav_p}\ \mu_0\right]Q_2 + \left[\frac{k_{tc}}{Nav_p}\right]\mu_0\mu_1 + \left[\frac{k_{td}}{Nav_p}\right]\mu_0\mu_1 \quad \text{(B21)}$$

$$k=2 \Rightarrow \frac{dQ_2}{dt} = +\left[\sum_{i=A,B} k_{fmi}[i]_{pol}\right]\mu_2 + \left[\frac{k_{fP}}{Nav_p}\ Q_1\right]\mu_2 - \left[\frac{k_{fP}}{Nav_p}\ \mu_0\right]Q_3 + \left[\frac{k_{tc}}{Nav_p}\right](\mu_0\mu_2+\mu_1^2) + \left[\frac{k_{td}}{Nav_p}\right]\mu_0\mu_2 \quad \text{(B22)}$$

$$\mu_1 = \frac{\left[\sum_{i=A,B} k_{pi}[i]_{pol}\right]Nav_p\mu_0 + \left[\sum_{i=A,B} k_{fmi}[i]_{pol}\right]Nav_p\mu_0 + [k_{fP}Q_2]\mu_0 + k_t\mu_0^2}{\left[\sum_{i=A,B} k_{fmi}[i]_{pol}\right]Nav_p + [k_{fP}Q_1] + k_t\mu_0} \quad \text{(B23)}$$

Manipulating the equations it is possible to reduce the system significantly to:

$$\frac{dQ_0}{dt} = +\left[\sum_{i=A,B} k_{fmi}[i]_{pol}\right]\mu_0 + \left[\frac{k_{tc}}{2Nav_p}\right]\mu_0^2 + \left[\frac{k_{td}}{Nav_p}\right]\mu_0^2 \quad \text{(B24)}$$

$$\frac{dQ_1}{dt} = \left[\sum_{i=A,B} k_{pi}[i]_{pol}\right]\mu_0 + \left[\sum_{i=A,B} k_{fmi}[i]_{pol}\right]\mu_0 + \left[\frac{k_{tc}}{Nav_p}\right]\mu_0^2 + \left[\frac{k_{td}}{Nav_p}\right]\mu_0^2 \quad \text{(B25)}$$

$$\frac{dQ_2}{dt} = +\left[\sum_{i=A,B} k_{pi}[i]_{pol}\right](2\mu_1+\mu_0) + \left[\sum_{i=A,B} k_{fmi}[i]_{pol}\right]\mu_0 + \left[\frac{k_{tc}}{Nav_p}\right]\mu_1^2 - \left[\frac{k_t}{Nav_p}\right]\mu_0^2 \quad \text{(B26)}$$

$$\mu_0 = \bar{n}N_p \quad \text{(B27)}$$

$$\mu_1 = \mu_1(\mu_0,\ Q_1,\ Q_2) \quad \text{(B28)}$$

$$\frac{dQ_0}{dt} = \frac{dQ_0}{dt}(\mu_0) \quad \text{(B29)}$$

$$\frac{dQ_1}{dt} = \frac{dQ_1}{dt}(\mu_0) \quad \text{(B30)}$$

$$\frac{dQ_2}{dt} = \frac{dQ_2}{dt}(\mu_0,\ Q_1,\ Q_2) = \frac{dQ_2}{dt}(\mu_0,\ \mu_1) \quad \text{(B31)}$$

The number average molecular weight, the weight average molecular weight and the polydispersity index are given by:

$$Mn = \frac{Q_1}{Q_0}(PM_Ay_A + PM_By_B) \quad \text{(B32)}$$

$$Mw = \frac{Q_2}{Q_1}(PM_Ay_A + PM_By_B) \quad \text{(B33)}$$

$$IP = \frac{Mw}{Mn} \quad \text{(B34)}$$

Appendix C. Kinetic constants and parameters used for the simulations

Table C.1: Kinetic constants used in the simulations (A, vinyl acetate/B, butyl acrylate).

Parameter	Value	Unit	Reference
k_i	$2.6\times10^{17}\exp(-3.3\times10^4/(1.987T))$	1/s	Penlidis, 1986
k_{pAA}	$6.14\times10^{10}\exp(-6.3\times10^3/(1.987T))$	cm^3/mol s	McKenna, Graillat & Guillot, 1995
k_{pBB}	$2.73\times10^{10}\exp(-6.3\times10^3/(1.987T))$	cm^3/mol s	McKenna et al., 1995

Parameter	Value	Unit	Reference
k_{fmAA}	$2.43 \times 10^{-4} k_{pAA}$	cm^3/mol s	Chatterjee, Park & Graessley, 1977
k_{fmBB}	$5.0 \times 10^{-8} k_{pBB}$	cm^3/mol s	Estimated
k_{fmAB}	$2.43 \times 10^{-4} k_{pAA}$	cm^3/mol s	Estimated
k_{fmBA}	$1.5 \times 10^{-5} k_{pBB}$	cm^3/mol s	Estimated
k_{fPA}	$2.36 \times 10^{-4} k_{pAA}$	cm^3/mol s	Chatterjee et al., 1977
k_{tAA}	$4.643 \times 10^{9} \exp(-2.8 \times 10^{3}/(1.987T))$	cm^3/mol s	McKenna et al., 1995
k_{tBB}	$1.68 \times 10^{7} \exp(-2.8 \times 10^{3}/(1.987T))$	cm^3/mol s	McKenna et al., 1995
k_{tAB}	$4.643 \times 10^{8} \exp(-2.8 \times 10^{3}/(1.987T))$	cm^3/mol s	McKenna et al., 1995
k_{tBA}	$4.643 \times 10^{8} \exp(-2.8 \times 10^{3}/(1.987T))$	cm^3/mol s	McKenna et al., 1995

obs, T in K.

Table C.2: Parameters used in the simulations (A, vinyl acetate/B, butyl acrylate).

Parameter	Value	Unit	Reference
a_S	3.43×10^{9}	cm^2/gmol	Ahmed, El-Aasser, Micale, Poehlein & Vanderhoff, 1971
CMC	1.846×10^{-3}	g/cm^3	Brandrup & Immergut, 1989
C_{pA}	$(3.621 + 6.676 \times 10^{-2} T - 2.103 \times 10^{-5} T^2 - 3.965 \times 10^{-9} T^3)/PM_A$	cal/g K	Reid, Prausnitz & Poling, 1987
C_{pB}	0.4142	cal/g K	Brandrup & Immergut, 1989
C_{pP}	0.35014	cal/g K	Brandrup & Immergut, 1989
C_{pW}	$(5.2634 \times 10^{4} + 2.4119 \times 10^{2} T - 0.85085 T^2 + 10^{-3} T^3) 0.2389 \times 10^{-3}/PM_W$	cal/g K	Reid et al., 1987
D_{wA}	1.1×10^{-5}	cm^2/s	Bird, Stewart & Lightfoot, 1960
D_{wB}	1.1×10^{-5}	cm^2/s	Bird et al., 1960
D_{pA}	1.1×10^{-6}	cm^2/s	Bird et al., 1960
D_{pB}	1.1×10^{-6}	cm^2/s	Bird et al., 1960
f_{mic}	50		Abad, 1995
j_{critA}	20		Tauer & Kühn, 1995
j_{critB}	8		Gilbert, 1995
k_A^d	34.7		Gardon, 1968
k_A^p	29.5		Gardon, 1968
k_B^d	705		Gugliotta, Arzamendi & Asua, 1995
k_B^p	460		Gugliotta et al., 1995
PM_A	86.09	g/gmol	Brandrup & Immergut, 1989
PM_B	128.17	g/gmol	Brandrup & Immergut, 1989
PM_E	288.38	g/gmol	Brandrup & Immergut, 1989
PM_I	225	g/gmol	Perry & Chilton, 1980
r_A	0.037		Gugliotta et al., 1995
r_B	6.35		Gugliotta et al., 1995
r_m	2.5×10^{-7}	cm	Rawlings & Ray, 1988
z_A	8		Gilbert, 1995
z_B	1		Gilbert, 1995
ρ_A	$0.9593 - 0.00134 T^*$	g/cm^3	Barudio, Févotte & McKenna, 1999
ρ_B	$0.9197 - 0.00104 T^*$	g/cm^3	Barudio et al., 1999
ρ_P	$(-0.1468 - 2.4 \times 10^{-3} T^*)(1 - y_A) + 1.2244 - 1.01 \times 10^{-3} T^*$	g/cm^3	Barudio et al., 1999
ρ_W	$PM_w 4.6 \times 10^{-4} (0.26(1 + (1 - T/647.29)^{0.23}))^{-1}$	g/cm^3	Reid et al., 1987
$-\Delta H_{pA}$	21.391	kcal/gmol	Brandrup & Immergut, 1989
$-\Delta H_{pB}$	18	kcal/gmol	Hamer, Akramov & Ray, 1981

obs, T in K; T^* in °C.

References

Abad, C. (1995). *Estudio del proceso de obtención en un reactor loop de copolímeros de características comerciales*. Ph.D. thesis, Universidad del País Vasco, Spain (in Spanish).

Ahmed, S. M., El-Aasser, M. S., Micale, F. J., Poehlein, G. W., & Vanderhoff, J. W. (1971). Rapid measurament of adsorption isotherms of emulsifiers on latex particles. In R. M. Fitch (Ed.), *Polymer colloids II*. New York: Plenum Press.

Araujo, O. (1997). *Copolimerização e terpolimerização em emulsão: trabalho experimental e estudo de aspectos relacionados à modelagem matemática do processo*. D.Sc. thesis, EPUSP, Brazil (in Portuguese).

Araújo, P. H. H., & Giudici, R. (2001). Efeito das condições de operação sobre os pesos moleculares nas reações em semi-batelada de copolimerização em emulsão de acetato de vinila e acrilato de butila. *Proceedings of sixth Congresso Brasileiro de Polímeros*. Gramado, Brazil (in Portuguese).

Arzamendi, G., Leiza, J. R., & Asua, J. M. (1991). Semicontinuous emulsion copolymerization of methyl metacrylate and ethyl acrylate. *Journal of Polymer Science Part A 29*, 1549–1559.

Barudio, I., Févotte, G., & McKenna, T. F. (1999). Density data for copolymer systems: butyl acrylate/vinyl acetate homo and copolymerization in ethyl acetate. *European Polymer Journal 35*, 775–780.

Bhaskar, V., Gupta, S. K., & Ray, A. K. (2001). Multiobjective optimization of an industrial wiped film poly(ethylene terephthalate) reactor: some further insights. *Computers and Chemical Engineering 25*, 391–407.

Bird, R. B., Stewart, W. E., & Lightfoot, E. N. (1960). *Transport phenomena*. New York: Wiley.

Bojkov, B., & Luus, R. (1994). Time-optimal control by iterative dynamic programming. *Industrial and Engineering Chemistry Research 33*, 1486–1492.

Bojkov, B., & Luus, R. (1996). Optimal control of nonlinear systems with unspecified final times. *Chemical Engineering Science 51* (6), 905–919.

Brandrup, J., & Immergut, E. H. (1989). *Polymer handbook* (3rd ed). New York: Wiley.

Canu, P., Canegallo, S., Morbidelli, M., & Storti, G. (1994). Composition control in emulsion copolymerization. I. Optimal monomer feed policies. *Journal of Applied Polymer Science 54*, 1899–1917.

Chatterjee, A., Park, W. S., & Graessley, W. W. (1977). Free radical polymerization with long chain branching: continuous polymerization of vinyl acetate in *t*-butanol. *Chemical Engineering Science 32*, 167–178.

Choi, K. Y., & Butala, D. N. (1991). An experimental-study of multiobjective dynamic optimization of a semibatch copolymerization process. *Polymer and Engineering Science 31*, 353–364.

Gardon, J. L. (1968). Emulsion polymerization. II. Review of experimental data in the context of the revised Smith–Ewart Theory. *Journal of Polymer Science Part A-1 6*, 643–664.

Gilbert, R. G. (1995). *Emulsion polymerization* (1st ed). London: Academic Press.

Gugliotta, L. M., Arzamendi, G., & Asua, J. M. (1995). Choice of monomer partition model in mathematical modelling of emulsion copolymerization systems. *Journal of Applied Polymer Science 55*, 1017–1039.

Gupta, R. R., & Gupta, S. K. (1999). Multiobjective optimization of an industrial nylon-6 semibatch reactor system using genetic algorithm. *Journal of Applied Polymer Science 73*, 729–739.

Hamer, J. W., Akramov, T. A., & Ray, W. H. (1981). The dynamic behavior of continuous polymerization reactors. 2. Non-isothermal solution homopolymerization and copolymerization in a CSTR. *Chemical Engineering Science 36*, 1897–1914.

Hansen, F. K., & Ugelstad, J. (1978). Particle nucleation in emulsion polymerization. I. A theory for homogeneous nucleation. *Journal of Polymer Science: Polymer Chemistry Edition 16*, 1953–1979.

Kozub, D. J., & MacGregor, J. F. (1992). Feedback control of polymer quality in semi-batch copolymerization reactors. *Chemical Engineering Science 47*, 929–942.

Leiza, J. R., de la Cal, J. C., Meira, G. R., & Asua, J. M. (1993). Online copolymer composition control in the semicontinuous emulsion copolymerization of ethyl acrylate and methyl methacrylate. *Polymer Reaction Engineering 1*, 461–498.

Luus, R. (1993). Application of dynamic programming to differential-algebraic process systems. *Computers and Chemical Engineering 17*, 373–377.

Luus, R. (1998). Iterative dynamic programming: from curiosity to a practical optimization procedure. *Control and Intelligent Systems 26* (1), 1–8.

Luus, R., & Rosen, O. (1991). Application of dynamic programming to final state constrained optimal control problems. *Industrial and Engineering Chemistry Research 30*, 1525–1530.

McKenna, T. F., Graillat, C., & Guillot, J. (1995). Contributions to defining the rate constants for the homo and copolymerisation of butyl acrylate and vinyl acetate. *Polymer Bulletin 34*, 361–368.

Omi, S., Kushibiki, K., Negishi, M., & Iso, M. (1985). Generalized computer modeling of semi-batch, n-component emulsion copolymerization systems and its applications. *Zairyo Gijutsu 3*, 426.

Penlidis, A. (1986). *Polymer reactor design, optimization and control in latex production technology*. Ph.D. thesis, McMaster University, Canada.

Perry, R. H., & Chilton, C. H. (1980). *Manual de engenharia química* (5th ed). Rio de Janeiro: Guanabara Dois.

Petzold, L. R. (1982). *A description of DASSL: a differential algebraic system solver*. Sandia National Laboratories, Report # SAND82-8637.

Rawlings, J. B., & Ray, W. H. (1988). The modeling of batch and continuous emulsion polymerization reactors: I. Model formulation and sensitivity to parameters. *Polymer Engineering Science 28* (5), 237–256.

Reid, R. C., Prausnitz, J. M., & Poling, B. E. (1987). *The properties of gases and liquids*. New York: McGraw-Hill.

Saenz de Buruaga, I. (1998). *Control en línea de reactores de polimerización en emulsión basado en medidas calorimétricas*. Ph.D. thesis, Universidad del País Vasco, Spain (in Spanish).

Saldivar, E., & Ray, W. H. (1997). Control of semicontinuous emulsion copolymerization reactors. *American Institute of Chemical Engineering Journal 43* (8), 2021–2033.

Santos, A. F., Sayer, C., Lima, E. L., & Pinto, J. C. (1999). Optimization of copolymerization reactions by iterative dynamic programming. *Proceedings of second Enpromer*, Florianópolis, Brazil.

Sayer, C., Arzamendi, G., Asua, J. M., Lima, E. L., & Pinto, J. C. (2001). Dynamic optimization of semicontinuous copolymerization reactions: composition and molecular weight distribution. *Computers and Chemical Engineering 25*, 839–849.

Tauer, K., & Kühn, I. (1995). Modeling particle formation in emulsion polymerization: an approach by means of the classical nucleation theory. *Macromolecules 28*, 2236–2239.

Tsoukas, A., Tirrell, M. V., & Stephanopoulos, G. (1982). Multiobjective dynamic optimization of semibatch copolymerization reactors. *Chemical Engineering Science 37* (12), 1785–1795.

Update

Computers and Chemical Engineering

Volume 28, Issue 4, 15 April 2004, Page 575–578

DOI: https://doi.org/10.1016/j.compchemeng.2003.08.006

Available online at www.sciencedirect.com
SCIENCE DIRECT®
Computers and Chemical Engineering 28 (2004) 575–578
Computers & Chemical Engineering
www.elsevier.com/locate/compchemeng

Corrigendum

Corrigendum to "Optimization of semicontinuous emulsion polymerization reactions by IDP procedure with variable time intervals" [Comput. Chem. Eng. 27 (2003) 1345–1360]☆

P. H. H. Araújo, R. Giudici*

Departmento de Engenharia Química, Escola Politécnica da Universidade de São Paulo, 380 travessa 3 Av. Prof. Luciano Gualberto, 05508-900 São Paulo, SP, Brazil

The author regrets that in the above article, some of the equations were incorrectly printed and an incomplete version of the Nomenclature was printed. The corrected equations and the complete Nomenclature will now follow.

$$\frac{\mathrm{d}(V_R[M_i])}{\mathrm{d}t} = q_e[M_i]_e - \frac{\tilde{n}N_P}{N_A}k_{pi}[M_i]_{pol} - [R_T]_{aq}V_{aq}k_{pi_{aq}}[M_i]_{aq} \tag{4}$$

$$y_A\frac{\mathrm{d}(V_R[P])}{\mathrm{d}t} = [P]\frac{\mathrm{d}(V_R y_A)}{\mathrm{d}t} - \frac{\tilde{n}N_P k_{pi}[M_A]_{pol}}{N_A} - [R_T]_{aq}V_{aq}k_{pi_{aq}}[M_A]_{aq} \tag{6}$$

$$[R_h]_{aq} = \frac{[R_{h-1}]_{aq}\sum_{i=A,B}k_{pi_{aq}}[M_i]_{aq}}{\sum_{i=A,B}k_{pi_{aq}}[M_i]_{aq} + \bar{k}_{t_{aq}}[R_T]_{aq} + (k_eN_P + k_{am}N_{mic})/V_RN_A} = [R_{h-1}]_{aq}\xi \tag{22}$$

$$\frac{\mathrm{d}[V_R\sum_{j=A,B,W,P}[M_j]C_{pj}(T_r - T_{ref})}{\mathrm{d}t} = \sum_{j=A,B,W} w_{j,e}q_eC_{pj,e}(T_e - T_{ref}) + \sum_{i=A,B}\left[\frac{\tilde{n}N_P}{N_A}(-\Delta H_{pi})k_{pi}[M_i]_{pol} + [R_T]_{aq}V_{aq}(-\Delta H_{pi})k_{pi_{aq}}[M_i]_{aq}\right] - U_jA_j(T_r - T_j) - Q_{lR} \tag{30}$$

$$C_{inst} = \frac{R_{pA}}{R_{pB}} = \frac{r_A([A]_{pol}/[B]_{pol}) + 1}{r_B([B]_{pol}/[A]_{pol}) + 1} \tag{33}$$

$$\beta = \frac{-(C_{inst} - 1) + \sqrt{(C_{inst} - 1)^2 + 4r_Ar_BC_{inst}}}{2r_BC_{inst}} \tag{34}$$

$$\frac{dR_1}{dt} = -R_l\sum_{i=A,B}k_{pi}[i]_{pol} - R_l\sum_{i=A,B}k_{fmi}[i]_{pol} - \left[\frac{k_{fP}}{Na\cdot v_p}\sum_{n=1}^{\infty}nM_n\right]R_1 + \left[\sum_{i=A,B}k_{fmi}[i]_{pol}\right]\sum_{n=1}^{\infty}R_n + \left[\frac{k_{fp}}{Nav_p}M_1\right]\sum_{n=1}^{\infty}R_n - \left[\frac{k_t}{Na\cdot v_p}\right]\sum_{n=1}^{\infty}R_nR_l + abs = 0 \tag{B1}$$

☆ doi of original article 10.1016/S0098-1354(03)00057-7.

* Corresponding author. Tel.: +55-11-818-5637; fax: +55-11-813-2380.
E-mail address: rgiudici@usp.br (R. Giudici).

doi:10.1016/j.compchemeng.2003.08.006

$$\left[\sum_{i=A,B} k_{pi}[i]_{pol}\right]\sum_{n=1}^{\infty}(n+1)^k R_n + \left[\sum_{i=A,B} k_{fmi}[i]_{pol}\right]\mu_0 + abs + \left[\frac{k_{fP}}{Nav_p}\sum_{n=1}^{\infty} n^{k+1} M_n\right]\mu_0$$
$$= \left[\sum_{i=A,B} k_{pi}[i]_{pol}\right]\sum_{n=1}^{\infty} n^k R_n + \left[\sum_{i=A,B} k_{fmi}[i]_{pol}\right]\sum_{n=1}^{\infty} n^k R_n + \left[\frac{k_{fp}}{Nav_p} Q_1\right]\sum_{n=1}^{\infty} n^k R_n + \left[\frac{k_t}{Nav_p}\right]\mu_0\sum_{n=1}^{\infty} n^k R_n \quad \text{(B5)}$$

$$k = 0 \Rightarrow \mu_0 = \sqrt{\frac{absNav_p}{k_t}} \quad \text{(B10)}$$

$$k = 2 \Rightarrow \mu_2 = \frac{\left[\sum_{i=A,B} k_{pi}[i]_{pol}\right] Nav_p(\mu_0 + 2\mu_1) + \left[\sum_{i=A,B} k_{fmi}[i]_{pol}\right] Nav_p\mu_0 + [k_{fP} Q_3]\mu_0 + absNav_p}{\left[\sum_{i=A,B} k_{fmi}[i]_{pol}\right] Nav_p + [k_{fP} Q_1] + k_t\mu_0} \quad \text{(B12)}$$

Nomenclature

Emulsion polymerization model

abs	rate of radical absorption into polymer particles (1/s)
A	vinyl acetate
A_j	heat transfer area (cm^2)
A_{pT}	total particle surface area (cm^2)
a_s	area covered by 1 g mol of emulsifier (cm^2/gmol)
B	butyl acrylate
C_{inst}	instantaneous copolymer composition ratio
CMC	critical micelar concentration (g/cm^3)
$C_{pj,e}$	specific heat of reactor fees streams (cal/(g K))
C_{pwj}	specific heat of cooling fluid (cal/(g K))
D_p	diffusion coefficient in the polymer particles (cm^2/s)
D_w	diffusion coefficient in the aqueous phase (cm^2/s)
$[E]$	concentration of emulsifier in the reactor (g/cm^3)
$[E]_{ads}$	emulsifier adsorbed on polymer particles (g/cm^2)
$[E]_{ads}^{sat}$	emulsifier adsorbed on polymer particles at saturation (g/cm^2)
$[E]_{aq}$	concentration of emulsifier in the aqueous phase (g/cm^3)
f	initiator efficiency
F_i	feed rate of monomer i to the reactor in (mol/s)
f_{kam}	efficiency of radical entry rate into micelles
f_{ke}	efficiency of radical entry rate into polymer particles
$[I]$	concentration of initiator in the reactor (g/cm^3)
i	amount of monomer i (A or B) in the reactor (mol)
i_0	amount of monomer i in the initial charge of the reactor (mol)
i_{pol}	amount of monomer i in polymer particles (mol)
$[i]_{pol}$	concentration of monomer i in polymer particles (mol/cm^3)
j_{crit}	critical length of radical (homogeneous nucleation)
k'	coefficient of emulsifier adsorption by polymer particles
k_{am}	radical entry rate into micelles (cm^3/(mol s))
k_e	radical entry rate into polymer particles (cm^3/(mol s))
k_{fi}	average rate constant for chain transfer of radical type i in the polymer phase (cm^3/(mol s))
k_{fit}	rate constant for chain transfer of radical type i to monomer j in the polymer phase (cm^3/(mol s))
k_{fP}	average rate constant for chain transfer to polymer in the polymer phase (cm^3/(mol s))
k_{fPi}	rate constant for chain transfer of radical type i to copolymer in the polymer phase (cm^3/(mol s))
k_i	rate constant for initiator decomposition (1/s)
$k^p i$	partition coefficient of monomer i between aqueous phase and polymer phase
k_{pi}	average rate constant for propagation of radical type i in the polymer phase (cm^3/(mol s))

k_{pij}	rate constant for propagation of radical type i in with a radical type j in the polymer phase (cm^3/(mol s))
k_{piaq}	average rate constant for propagation of radical type i in the aqueous phase (cm^3/(mol s))
k_t	average rate constant for termination in the polymer phase (cm^3/(mol s))
k_{taq}	average rate constant for termination in the aqueous phase (cm^3/(mol s))
k_{tif}	rate constant for termination of radical type i with radical type j in the polymer phase (cm^3/(mol s))
$[M_i]$	concentration of monomer i (A or B) in the reactor (g/cm^3)
$[M_i]_{aq}$	concentration of monomer i in the aqueous phase (g/cm^3)
$[M_i]_{pol}$	concentration of monomer i in the polymer phase (g/cm^3)
$\tilde{n}$	average number of radicals per polymer particle
N_A	Avogrado's number
N_{mic}	number of micelles
N_p	total particle number
$[P]$	concentration of polymer in the reactor (g/cm^3)
P_{Ap}	relative frequency of radicals presenting a monomeric unit of type A on its active end
P_{Bp}	relative frequency of radicals presenting a monomeric unit of type B on its active end
PM_E	molecular weight of the emulsifier (g/g mol)
q_e	inlet flow rate of the reactor (cm^3/s)
q_{je}	inlet flow rate of the jacket (cm^3/s)
q_{js}	outlet flow rate of the jacket (cm^3/s)
Q_{lj}	jacket heat loss to the surroundings (cal/s)
Q_{lR}	reactor heat loss to the surroundings (cal/s)
r_i	reactivity ratio of monomer I
r_m	radius of a micelle (cm)
r_{ps}	radius of a swollen polymer particle (cm)
$[R_h]_{aq}$	concentration of radicals with length h in the aqueous phase (mol/cm^3)
$[R_{jcrit}]_{aq}$	concentration of radicals of length j_{crit} in the aqueous phase (mol/cm^3)
R_{pi}	polymerization rate of monomer i (mol/s)
$[R_T]_{aq}$	total concentration of radicals in the aqueous phase (mol/cm^3)
$[R_T^{ent}]_{aq}$	concentration of radicals in the aqueous phase that can enter into a micelle or into a polymer particle (mol/cm^3)
t	time (s)
T_j	jacket temperature (°C)
T_{je}	jacket inlet temperature (°C)
T_r	reactor temperature (°C)
T_{ref}	reference temperature (°C)
U_j	global heat transfer coefficient (cal/(s cm^2 K))
V_{aq}	volume of the aqueous phase (cm^3)
V_{pol}	volume of the polymer phase (cm^3)
V_R	volume of the reactor (cm^3)
$[W]$	concentration of water in the reactor (g/cm^3)
W_j	amount of cooling fluid in the jacket (g)
$w_{j,e}$	weight fraction of component j in the reactor inlet feed stream
xg	global monomer conversion
xi	instantaneous monomer conversion
y_A	copolymer composition (molar fraction of VA in the copolymer)
z	minimum length of radical for radical entry into micelles and polymer particles

Greek letters

β	amount of emulsifier per micelle (g)
ΔH_{pi}	heat of polymerization of monomer i (cal/g)
θ_{ad}	fraction of polymer surface area covered by the emulsifier

Optimization procedure

A	number of random values of manipulated variables
F	objective function

$iter$	number of optimization iterations
Mn_f	final number average molecular weight
Mn_f^d	desired final number average molecular weight
Mw_f	final weight average molecular weight
Mw_f^d	desired final weight average molecular weight
N	number of time intervals of monomer feed period
P	number of time intervals after monomer feed period
r_i	size of search area of manipulated variable i
t_f	final reaction time (s)
t_d^f	desired final reaction time (s)
T_{ad}	total adiabatic temperature (°C)
T_{rd}	desired reactor temperature (°C)
$\underline{u}$	vector of manipulated variables
w	weight factors of the objective function
$\underline{x}$	vector of state variables
xg_f	final global monomer conversion
xg_f^d	desired final global monomer conversion

Greek letters

α_i	lower limit of manipulated variable i
β_i	upper limit of manipulated variable i
γ	contraction factor of search area